

Programming and Deployment of Autonomous Swarms using Multi-Agent Reinforcement Learning

Jayson Boubin
boubin.2@osu.edu
Ohio State University
Columbus, Ohio, USA

Codi Burley
burley.66@osu.edu
Ohio State University
Columbus, Ohio, USA

Peida Han
han.1242@osu.edu
Ohio State University
Columbus, Ohio, USA

Bowen Li
li.7652@osu.edu
Ohio State University
Columbus, Ohio, USA

Barry Porter
b.f.porter@lancaster.ac.uk
Lancaster University
Lancaster, United Kingdom

Christopher Stewart
cstewart@cse.ohio-state.edu
Ohio State University
Columbus, Ohio, USA

Abstract

Autonomous systems (AS) carry out complex missions by continuously observing the state of their surroundings and taking actions toward a goal. Swarms of AS working together can complete missions faster and more effectively than single AS alone. To build swarms today, developers handcraft their own software for storing, aggregating, and learning from observations. We present the Fleet Computer, a platform for developing and managing swarms. The Fleet Computer provides a programming paradigm that simplifies multi-agent reinforcement learning (MAREL) – an emerging class of algorithms that coordinate swarms of agents. Using just two programmer-provided functions *Map()* and *Eval()*, the Fleet Computer compiles and deploys swarms and continuously updates the reinforcement learning models that govern actions. To conserve compute resources, the Fleet Computer gives priority scheduling to models that contribute to effective actions, drawing a novel link between online learning and resource management. We developed swarms for unmanned aerial vehicles (UAV) in agriculture and for video analytics on urban traffic. Compared to individual AS, our swarms achieved speedup of 4.4X using 4 UAV and 62X using 130 video cameras. Compared to a competing approach for building swarms that is widely used in practice, our swarms were 3X more effective, using 3.9X less energy.

1 Introduction

Autonomous systems (AS) continuously sense their surroundings, model their current state and take actions toward a goal. Edge computing, a paradigm where compute resources are provisioned near sensing devices, has propelled AS in a wide range of industries [5, 23, 41, 68].

Groups of AS working toward a common goal are called *swarms*. Compared to AS working alone, swarms can speed up mission execution. First, missions can be partitioned into tasks that swarm members execute in parallel. Second, swarm members can share observations of their surroundings to help other members take effective actions. Today, human programmers manually partition missions for swarm operations and each swarm member uses pre-programmed

behaviors. For example, in precision agriculture, such *automated swarms* divide a crop field among multiple UAV and each UAV executes pre-programmed scouting routines on its region [3]. Recent research provides automated partitioning and fault tolerance for automated swarms [23]. However, pre-programmed behaviors fundamentally waste resources by collecting and processing data of low value relative to the mission. Further, by limiting autonomy, data sharing between members can not improve efficacy.

Multi-Agent Reinforcement Learning (MAREL) is an emerging class of reinforcement learning algorithms where agents cooperate to maximize a reward. Agents learn their own reinforcement-learning policies, but they can also learn from the actions and outcomes of other agents. MAREL algorithms applied to AS swarms can speedup missions via partitioning (like the automated approach above) and via efficacy (i.e., taking better actions). Further, recent research on MAREL algorithms provides provable guarantees and strong empirical results [8, 11, 32, 63]. However, MAREL systems are not simple to develop and manage; they require infrastructure for AS workflows, selecting MAREL algorithms and reward functions, and data management policies. Developers must create this infrastructure by hand and incorporate it into a real-world system. The result is that, despite their potential, these algorithms rarely go beyond theoretical studies or highly specialised applications with bespoke components.

We present the *Fleet Computer*, a platform for developing and managing MAREL-driven swarms. To program AS in the Fleet Computer, developers provide two functions: *Map()* and *Eval()*. *Map()* converts sensed observations (e.g., images) to application-specific feature vectors. *Eval()* evaluates system performance towards autonomy goals. In addition, developers also provide hardware resources and mission configuration settings, e.g., allowed actions and goals. With these inputs, the Fleet Computer compiles MAREL models that govern autonomous actions. Then, during execution, the Fleet Computer aggregates data from swarm members and re-trains the models governing actions. However, retraining stresses limited computational resources at edge sites. The

Fleet Computer prioritizes retraining for models most useful for effective actions, making a novel link between online learning and resource management. The Fleet Computer also expands and contracts edge compute resources via duty cycling to save energy and reducing over provisioning.

Just as MapReduce [13] simplified parallel data processing, the Fleet Computer demystifies fully autonomous swarms. In addition to its novel programming paradigm, the Fleet Computer provides end-to-end control, deployment, and scheduling of an entire swarm-support infrastructure – from individual swarm units, such as a UAV, to the supporting heterogeneous compute resources at the edge.

The Fleet Computer comprises 3 main contributions:

1. A programming model and toolchain that allows users to easily build MARL-driven swarms.
2. A novel, online-learning approach to aggregate observations from swarm members and dynamically update models governing actions.
3. A runtime platform that manages, schedules and duty-cycles edge compute resources, simplifying deployment.

We used the Fleet Computer to build both aerial crop scouting and video analytics systems, demonstrating its broad applicability to significantly different problems. We developed a swarm of unmanned aerial vehicles used to predict crop yield from flyover images. We also developed a taxicab tracking workload using a swarm of autonomous cameras. By providing a simple way to take advantage of state-of-the-art MARL algorithms, our crop yield mapping application outperforms state of the art yield mapping, improving mapping times by 4.4X using 3.9X less UAV power. Similarly, our vehicle tracking workload built using the Fleet Computer outperforms prior work, tracking taxis up to 62X faster as a swarm compared to centralized processing while maintaining good performance over time by updating models regularly. Using these applications, we demonstrate that a compute cluster running Fleet Computer software can easily scale up from a single UAV, camera, or other agent to a complete swarm that can learn from its actions while dynamically allocating resources to fit demand and save precious power at the edge.

The remainder of the paper is organized as follows: Section 2 describes at a high level the overarching design of the Fleet Computer. Section 3 details our programming model, which allows users to easily build autonomous swarms that perform well. Section 4 discusses the Fleet Computer’s runtime, which includes a priority-based online learning approach to maintain model performance as environments change, and cluster autoscaling which saves edge power without sacrificing performance. Section 5 covers two Fleet Computer implementations: video analytics and autonomous crop scouting. Section 6 presents results for the Fleet Computer on both applications. Section 7 presents related work and Section 8 provides conclusions.

2 Background

Self-driving cars [33, 56], UAV [6, 48, 62], and other autonomous systems (AS) [7, 16, 44, 52] are transforming society. Investments in self-driving cars exceed \$56B [36]. UAV are transforming delivery, infrastructure monitoring, and surveillance [1, 2, 6, 23, 50]. Autonomous cameras with mobile gimbals are powering traffic monitoring and smart cities [24]. In this paper, the term *autonomous* describes systems that sense their surroundings, infer their state, and take actions toward mission goals *without human intervention*.

By design, AS execute in unfamiliar surroundings. Their efficacy depends on how well their actions align to mission goals. Broadly, AS can be characterized by two key design choices: (1) Do they learn from their own observations? And (2) do they learn from the observations of other AS? For many AS used in practice today, the answer to both questions is no. These *pre-programmed AS* repeat the same routine across all missions, often taking unneeded and wasteful actions.

With reinforcement learning, AS can learn from prior observations [6, 15, 26, 33, 48]. However, often in practice, AS observe the world too slowly to capture enough data for learning, especially in non-stationary contexts where the best actions change. Multi-agent reinforcement learning (MARL) addresses this problem by aggregating data from multiple AS (i.e., swarms). Previously, the challenge for MARL-driven AS has been deciding from which swarm members to learn, but recent research has developed online algorithms to explore data aggregations that have provable guarantees and/or strong empirical results [8, 11, 32, 63]. However, even with recent research, swarms require additional compute resources compared to single-agent AS. To share data, swarms members must be networked, e.g., via hubs [4, 57] or wireless [22, 58]. Exploring data aggregations also requires additional compute resources.

Autonomous UAV for Crop Yield Modeling: To illustrate these concepts, consider a farmer that owns 4 UAV controlled via apps running on 4 tablets. The tablets and an edge-hub desktop share a wireless Internet connection. The mission is to map the expected crop yield for each $0.01 \times$ acre lot in a 1,000 acre field with accuracy above 80%. For the approach most commonly used in practice, the farmer would use pre-programmed routines to exhaustively capture images from 100,000 waypoints. This approach is slow and unnecessarily exceeds accuracy goals. A pre-programmed swarm could split the mission into 4 parallel tasks. With reinforcement learning, AS can visit significantly fewer waypoints [5, 48, 66] by continuously modeling the expected accuracy of their map and prioritizing valuable waypoints to visit next. MARL-driven AS improve upon naive reinforcement learning by using shared images to visit fewer waypoints. However, the computational load for reinforcement learning and MARL exceeds the capacity of UAV processors and tablets, requiring resources of an edge hub or the cloud.

3 Design

As shown in Figure 1, the Fleet Computer is an end-to-end platform for autonomous swarms, covering the development of AS, their workflow and coordination, and their execution on edge computing devices.

To create an AS, developers implement two functions, Map() and Eval(), and specify mission configuration. Map() functions convert quantized input from sensing devices (e.g., cameras, GPS, etc.) into a feature vector that represents the state of the AS. Eval() functions aggregate all outputs from Map() invocations during an epoch and assess the extent to which the mission has been completed. The mission configuration defines key parameters that developers can adjust across swarm applications. Figure 1 depicts three examples of mission configuration settings. First, developers can provide thresholds to determine when missions are complete. By default, the Fleet Computer supports thresholds on accuracy and energy usage. Second, developers specify the type of resources needed for sensing, processing, and data aggregation by stipulating quantitative requirements, such as CPU and memory required for Map() execution. Third, users provide qualitative requirements, such as support for specific Action Drivers. Action Drivers support a cyber-physical system’s actions, e.g., take off, land, sense, and fly to waypoint.

The Fleet Computer compiles these inputs to create AS workflows for sensing surroundings and taking actions. Here, the challenge is to decide which actions to take after running Map() and Eval(). The Fleet Computer automatically builds state-to-action (SA) models and history-to-action (HA) models by (1) replaying data from prior execution contexts, and (2) learning effective actions that improve Eval() outcomes. SA models convert a single map output to actions whereas HA models convert multiple observed outputs.

The Fleet Computer models MARL-driven AS as three asynchronous components: Sensors, AS Workflow, and Data Aggregation. These components execute in shared-nothing containers connected via distributed storage (e.g., HDFS [51]). Containers are replicated to support swarms. Precisely, a swarm of size N will comprise N Sensor and AS containers and up to 2^N Data Aggregation containers (representing every possible combination of aggregations). Clearly, Data Aggregation containers impose computational demands that exceed system capacity— a challenge common to all MARL-driven approaches [8, 32, 63]. For small swarms ($N \leq 8$), The Fleet Computer deploys all Data Aggregation containers and employs a novel, priority-based online learning and scheduling to manage compute demand. For larger swarms, the Fleet Computer supports developer-provided heuristics to limit aggregation.

In this section, we first provide a rigorous primer on MARL algorithms. Then, we introduce the specification of Fleet Computer applications, i.e., swarms of AS. Finally, we describe each of the key functions and models listed above.

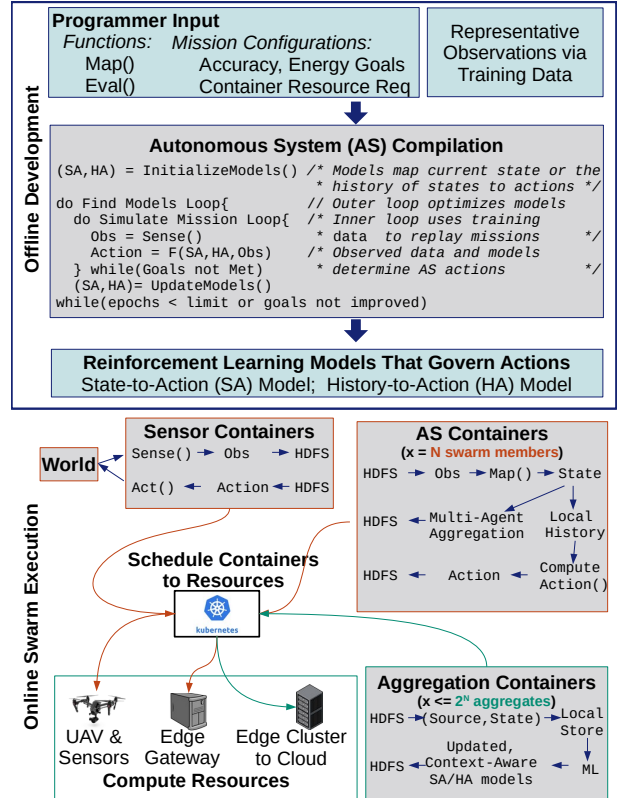


Fig. 1. The architecture of the Fleet Computer.

3.1 MARL Primer

Broadly, reinforcement learning approaches determine a policy π^* that approximates an optimal solution to a Markov Decision Process (MDP). MDPs comprise States S , Actions A , a transition probability function $P \rightarrow S \times A \rightarrow \Delta(S)$, a reward function $R(s_i, a_i, s_{i+1})$ defining the immediate reward an agent receives from performing an action, and a discount factor γ [64]. A policy π is a means of determining which action to take in a given state to transition to another state. The optimal policy π^* is the policy that results in the set of state transitions that maximizes overall reward.

$$MDP : (S, A, P, R, \gamma) \quad (1)$$

MDPs are a useful tool for solving simple state transition problems, but fleet missions are too complex for this framework. Consider the crop yield modeling example from Section 2. Crop scouting is a complex workload where the execution context changes over time and reward is difficult to define. If the system is rewarded based on the estimated yield it predicts in each state, it will likely over or under-predict yield based on how reward is assigned. Furthermore, even if reward is properly assigned, it is likely that states and transition probabilities will change over time as crops grow and conditions change. In many cases, an optimal policy is nearly impossible to determine a priori. For these tasks,

reinforcement learning is used to develop $\pi^{*'} \approx \pi^*$, an approximately optimal policy for navigating execution contexts while maximizing reward.

There are many methods for approximating π^* through reinforcement learning including value based methods like Q-learning, policy based methods like actor-critic RL, and analogous deep methods like Deep Q-Networks and Deep Deterministic Policy Gradients [20, 31, 39, 59]. Throughout this paper, we will use Q-learning as a basis for MARL, but other techniques fit into our programming model as well. Q-learning is a value-based method for reinforcement learning which uses a Q-function to determine $\pi^{*'}$. $Q(S_i, A_i)$ is the Q-function which predicts the expected value (Q-value) of an action A_i taken at state S_i . In practice, Q-values are stored in a Q-table $Q[S, A]$ indexed by state-action pairs. When an action is performed, the Q-table is updated using the bellman equation shown in equation 2, which uses dynamic programming to update the Q-value for a state-action pair based on the reward for a given action, plus expected reward of all future actions modified by learning rate α and discount factor γ . Properly informed Q-tables and other RL mechanisms solve MDPs with high accuracy by learning $\pi^{*'}$, allowing them to learn complex behaviors through exploration.

$$Q(s_i, a_i) = (1 - \alpha) * Q(s_i, a_i) + \alpha [R(s_i, a_i, s_{i+1}) * \gamma \max(Q(s_{i+1}, a_{i+1}))] \quad (2)$$

This process translates quite well to multi-agent systems. Transitioning a reinforcement learning algorithm to a multi-agent domain can involve constructing careful global reward functions [10]. Another approach, team-average reward [14, 25], maximizes the reward received by the system given agents with different and potentially discordant reward functions. MARL algorithms of this type are called Markov Games (MGs) [35]. MGs, shown in equation 3, expand the MDP by adding multiple agents, defined by $N \geq 1$. Each agent $i \in N$ has its own action set A_i and reward function R_i . Similar to MDPs, the solution to the MG is policy π^* , the set of state transitions that maximizes reward. Much work has also been done with networked agents [46, 63, 65], agents within a MG that communicate over some time-varying network, may have individual reward functions, and may require data privacy.

$$MG = (N, S, A_{i \in N}^i, P, R_{i \in N}^i, \gamma) \quad (3)$$

Given this specification, the Fleet Computer should accommodate different MARL algorithms using the same base components while assuring that these algorithms fit within the fleet framework. To allow the design and deployment of MARL algorithms for real-world AS, the Fleet Computer takes some of these base MARL components as inputs and generates others offline.

3.2 The FleetSpec

$$FleetSpec : (N, S, A_{i \in N}^i, Map(), Eval(), \mathbb{C}) \quad (4)$$

Equation 4 presents the minimum specification for Fleet Computer applications, called the FleetSpec. Similar to a Markov Game, the FleetSpec accepts a number of agents $N \geq 1$, states S , and action sets A_i for each agent. States are non-injective and surjective mappings from action sequences to integers $\langle a_{t=0}^t, a_{t=1}^t \dots a_{t=T}^t \rangle \rightarrow \mathbb{Z}$ where $a^t \in A_{i \in N}^i$. States affect the behavior of action drivers. For example, if a vehicle is at the eastern edge of allowed states, the command *go East* is muted by the action driver. Unlike Markov Games, FleetSpec eschews state transition probability and reward functions. First, Fleet Computer developers can reuse action drivers created by others. The action drivers may support states about which the developers are unaware, making state transition models incomplete. Second, constructing mathematical reward functions is challenging. Real-world AS take on missions that involve complex, domain-specific knowledge. The value of their actions can be subtle and may depend on prior actions, requiring complex non-linear reward functions that overly complicate the development of AS.

Instead, the Fleet Computer learns state-to-action (SA) models and history-to-action models (HA) automatically through training and reward shaping. These models represent an approximation of $\pi^{*'}$. The Map() and Eval() functions, coupled with representative observations from prior missions \mathbb{C} , suffice to compile initial MARL models and reward functions. The remainder of this section details the compilation process.

3.3 Map() and Eval() Functions

Like in MapReduce, Map() functions in the Fleet Computer structure input data. AS get their input data from sensor containers. The output is a feature vector, called a state-space vector (SSV), that describes sensed observations in the system's current state. Precisely, let D_j be the sensor data observed in state S_i , $Map(D_j)$ directly translates observed sensor data to a SSV, as shown below.

$$D = \langle d_1, d_2, \dots, d_n \rangle \quad (5)$$

$$Map(D) = SSV = \langle f_1, f_2, \dots, f_m \rangle \quad (6)$$

By emitting a structured SSV, Map() functions in the Fleet Computer can compose multiple *extractor functions* that process a portion of the sensed data $D' \subset D$ and emit part of the SSV. Extractor functions are shown in Figure 2 for our crop scouting example. $Map(D_j)$ for crop scouting provides data D_j to extractors including $ExG()$ which determines excess green [28] (a metric for predicting crop yield), $LAI()$ which estimates the leaf area index [47] of crops in the image, and a CNN which counts the number of corn stalks in the image among other extractors. Each of these extractors provides important information about the execution context that can be used to both build final yield maps and predict optimal actions for sampling. Each of these extractors return one or more floating point values which are added to the final SSV.

```

1  func[] extractors = [ExG(), LAI(),
2                        CornCountCNN(), ...]
3  float[] Map(Obj data) {
4      float[] SSV = [];
5      for(e in extractors) {
6          SSV.append(e(data));
7      }
8      return SSV;
9  }
10
11 Obj[] Eval(float[][] FS, float[][] perf) {
12     finished = checkGroups(FS, HA)
13     map_final = []
14     if(finished) {
15         map_gt = buildMap(FS)
16         map_final = extrap(map_gt)
17     }
18     P = buildMetrics(perf)
19     return [finished, P, map_final]
20 }

```

Fig. 2. Map and Eval function pseudocode for crop scouting.

Eval() determines whether and to what degree an AS has accomplished its goal. For some AS, this can be as simple as reaching a certain state. For others, like the autonomous crop scouting example, goal evaluation is more difficult. Depending on the size and type of field being modeled, the goal may be to make the most accurate yield map possible within some timeframe, cost, or sampling coverage.

$$FS = \{SSV_1, SSV_2, SSV_3 \dots SSV_n\} \quad (7)$$

$$P = \{\rho_1, \rho_2, \rho_3 \dots \rho_m\} \quad (8)$$

$$Eval(FS, m) = P \quad (9)$$

Eval(), defined above, accepts a feature space FS comprised of $n \geq 1$ SSVs and a set of system-level metrics m , and outputs an evaluation P which includes $x \geq 1$ evaluation metrics $\rho_1 \dots \rho_m$. The number of state-space vectors and evaluation metrics required is task and goal dependant.

For our crop scouting UAV example, many or all sensed SSVs from a mission may be needed to build an accurate yield map. Evaluation metrics for crop scouting may include system execution time, accuracy, energy expenditure, monetary cost and any other metric that determines real-world performance. Eval() pseudocode for crop scouting is shown in Figure 2.

Eval accepts two parameters, a featureset of all SSVs collected by the system, and a set of performance metrics for each agent. First, we use the HA model to determine whether the mission has concluded by exploring all state groups, a process detailed in section 3.4. If the mission is finished, a final yield map is generated by converting FS into a ground-truth yield map by mapping ExG from each SSV into a yield

Name	Linkage	Data Type	Devices	Use-Cases
Point clouds	Spatial	RGBD, ASCII	Robots	Indoor and outdoor Navigation
Video streams	Spatial, Temporal	Video	Self-driving cars, Video analytics	Transportation, Tracking,
Autonomy cubes	Spatial, Temporal	Images, Video	UAV	Precision agriculture, Rescue, Photography

Table 1. Execution context data sets and their use cases.

prediction and mapping it onto the execution context. Then, unvisited zones are extrapolated using an approach from prior work [66]. Next, Eval() uses performance metrics from every agent to build a set of global metrics that can be used for goal evaluation, P . Finally, Eval() returns a Boolean stopping condition based on HA, evaluation metrics, and potentially a final yield map which will be returned to the user.

3.4 State-To-Action and History-To-Action Models

Designing MARL policies and reward functions is a complicated problem with many situational solutions. Each action taken by an agent must be assessed by a policy before it is selected, and assigned reward if it is taken. The Fleet Computer’s model training and reward shaping steps simplify this process, allowing users without predefined models or reward functions the option to build them automatically.

Training reinforcement learning policies generally requires releasing an agent into an execution context and allowing it to explore, building a policy using a reinforcement learning model from the reward it garners from its actions. Characterizing entire real-world execution contexts for training models is a well-explored problem. Point-cloud datasets have long been used in robotics and computer vision for simulating navigation and robotic manipulation in real-world environments [12, 43, 53, 55]. Data sets for self-driving vehicles [19, 27, 61] and video analytics [42, 67] provide labeled video streams of fully explored environments used to train algorithms in both domains. A similar approach, Autonomy Cubes, provides spatially and temporally linked images in the form of hypercubes representing completely explored execution contexts regularly used to develop autonomous UAV workloads [6, 60, 66].

Any of these execution context representations can be used to train MARL models for the Fleet Computer. In the FleetSpec, these execution contexts are defined as \mathbb{C} . Map() and Eval() combined with autonomy goals allow agents to navigate these environments just like the real world, with Map() extracting data from a given state, and Eval() determining whether autonomy goals are sufficiently accomplished. These functions do not, however, constitute a policy. The

policy for navigating these environments is defined by State-to-Action and History-to-Action models detailed below.

A State-to-Action model (SA) is a blank or pretrained MARL model $SA \approx \pi^*$. SA accepts a SSV as input and returns an action. SA is not strictly tied to any RL or MARL model format, and is meant to be general. By default, the Fleet Computer supports Q-learning, but other model types, like DQNs or DDPGs can be substituted as an SA baseline. SA can also be provided pre-trained, or the Fleet Computer can instantiate it from a blank model and train it with data from \mathbb{C} . The only restriction placed on SA by the Fleet Computer is that it must accept an SSV produced by Map() as an argument.

History-to-Action() models provide spatial support to SA models. An HA model determines if an AS has accomplished its goal within its execution context. As an AS explores its execution context, some states of low relevance can be excluded or extrapolated to conserve time, energy, and compute resources. MARL models generally rely solely on reinforcement learning to determine which states to search, but recent video analytics work [24] demonstrates how spatial and temporal correlations can help prune search spaces effectively. In response to this work, we propose that groups of states (state groups) be allocated in conjunction with HA models to better search across execution contexts.

A state group is a collection of states within the execution context, with each state belonging to one or more state groups. State groups provide spatial bounds on AS. Often, phenomena sought by AS is spatially correlated [24, 66]. By defining spatial bounds, AS can limit their searches, saving time and resources. HA determines the number of states explored in each group. After a state in the state group is visited, the feature vectors of each visited state in that group are provided to HA to determine whether to explore another state in that group, or to visit another group. If the system decides to visit another state group, all unexplored zones in the group are either disregarded or predicted by Eval(). HA is defined as follows.

$$HA(FS) = \begin{cases} U > T_u \text{ or } V > T_v & 0 \\ \text{else} & 1 \end{cases} \quad (10)$$

$$U = \sum_{i=0}^n R(S_i, A_i, S_{i+1}) \quad (11)$$

$$V = \|FS\| \quad (12)$$

HA accepts a feature space FS comprised of one or more state-space vectors $SSV_1..SSV_n$ from the same state group. $HA(FS)$ returns a Boolean value representing whether to continue exploring a state group (0) or to move on and explore another (1). This decision is made using U , the total utility of the feature space, and V , the size of the feature space (number of visited states in the group). The utility of a feature space is the aggregate reward received from all state transitions within that space. If U is above T_u , the utility

threshold, or V is above T_v the visited states threshold, all remaining states in the group are ignored or predicted by Eval() and another state group is visited. The two thresholds strike a balance between allowing the MARL algorithm time to find high reward state transitions and limiting the total number of states visited to maintain efficiency.

These thresholds, as well as the means for determining reward, are difficult to determine a priori. Rigorous construction of high-quality reward functions is still an open problem, and could be difficult for users attempting to apply autonomy to a new domain or in an unclear application [29, 64, 69]. Work has been done on reward shaping [21, 34, 69], but there is still no best practice on how reward functions should be developed. We take inspiration from recent work that used meta-learning via gradient descent to construct reward functions [69]. Because our Map() functions have smaller numbers of features, we can define a rigorous means for estimating optimal reward functions and thresholds through a simpler and faster technique, Bayesian optimization [18].

3.5 Reward Shaping and Training

Provided one or more execution context data sets, Map() and Eval() functions, and SA, our algorithm initializes hyperparameter values for the reward function and HA thresholds, then simulates autonomous missions over each execution context, and evaluates performance. We use bayesian optimization [18] to find a goal-maximizing combination of Reward, SA, and HA.

$$R(S_i, A_i, S_{i+1}) = \sum_{i=0}^n S_{i+1}^n * w_n \quad (13)$$

Reward, shown above, is the sum of each normalized feature of S_{i+1} multiplied by its corresponding weight w_i . Weights are a feature specific hyperparameter between 0 and 1. Using these properties, we can determine that the output of $R(S_i, A_i, S_{i+1})$ will be in the range $[0, \|F_i\|]$. For this reason, T_u may only fall in the same range. Similarly, T_v must be an integer value between $[0, V]$. Through simulation, Bayesian optimization tunes these values until user-specified accuracy and energy requirements are met.

Bayesian optimization is a function approximation technique that minimizes or maximizes objective functions with many parameters through creatively searching their state-space [18]. Users must provide a set of defined autonomy goals $G = \{g_1, g_2, ..g_n\}$ corresponding with outputs of the Eval() function. Using G we can construct a multi-variate loss function which serves as the objective function for Bayesian optimization.

Figure 4 shows our Bayesian reward shaping process in pseudocode. Our buildReward function accepts 4 parameters: the number of features from Map() to be weighted, the subsetset of contexts to be simulated across \mathbb{C}_t , the number of training epochs, and the list of autonomy goals G . Before

```

1  float[] buildReward(int nFeats, Obj[] C,
2     int numEpochs, float[] G) {
3     float[] W = initWeights(nFeats)
4     int T, T* = GROUP_SIZE
5     int V, V* = MAX_INT
6     int bestLoss = MAX_INT
7     float[] maxWeights = []
8
9     for i in range(numEpochs){
10        float loss = 0
11        for con in C{
12            float[] e = sim(con,W,T,V)
13            loss += F(G, e)
14            if(loss < bestLoss and goalsMet(G, e)]
15                bestLoss = loss
16                maxWeights, T*, V* = W, T, V
17            W, T, V = Bayes([W, T, V], loss)
18        }
19    return maxWeights;
}

```

Fig. 3. Bayesian reward shaping pseudocode. Reward Shaping seeks to find the set of hyperparameters which minimizes loss and meets goals.

training, weights and thresholds are initialized. Training consists of simulating missions using each context $c \in \mathbb{C}_r$. Loss is calculated based on autonomy goals G and the final simulation evaluation $e \forall con$ using objective loss function $F(e, G)$. The additive loss for all cubes is then compared to the best prior loss. If loss is less than the best previous loss and all goals are met, the hyperparameters are saved. When the last training epoch concludes, the hyperparameters with the least additive loss that met all goals are returned, providing complete HA and reward functions.

Once reward shaping has concluded, SA is retrained with a separate subset of contexts \mathbb{C}_r using a similar process. Missions are simulated across \mathbb{C}_r with the new reward function and evaluated against prior training examples to select the best combination. The number of retraining periods for both SA and reward shaping are specified by user-defined hyperparameters.

4 Runtime

Using our goal-based development techniques for AS, users can more easily develop and train MARL algorithms for their individual problems. Output SA models may, however, be insufficiently trained to operate well in specific deployments. To help build high quality systems with limited initial training data, and allow algorithms to adapt to dynamic environments, we introduce a federated online learning system for MARL algorithms within the Fleet Computer. This system allows SA and HA models for individual swarm members to

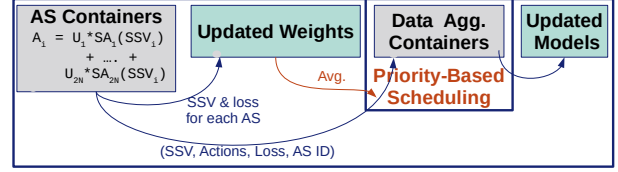


Fig. 4. Online learning provides coefficients for priority-based scheduling to update MARL models.

diverge to maximize global reward. Using an online learning component also introduces a scheduling and resource management problem domain for executing online learning tasks at the edge. In this section we first describe our federated learning approach to MARL for AS which uses Bayesian optimization to determine model usefulness for efficient retraining. We then present our runtime scheduling and resource management system for these online learning tasks, aided by Kubernetes.

4.1 Bayesian optimization for system-level hyperparameters

When a swarm is deployed, each member uses the original model SA for pathfinding decisions. As missions complete, swarm members' future performance may benefit from retraining using the the data they sense. It is unclear, however, whether retraining will immediately help or hurt performance, and which data should be used for maximum retraining performance. To solve these problems, we retrain a set of models SA_s using different subsets of collected data and weight their performance for every system.

Our solution to this problem is depicted in Figure 4. After a deployment's first mission, each swarm member has sensed and stored new data that can be used by aggregation containers for retraining. The sensed data can be partitioned into an infinite number of subsets to retrain $SA \rightarrow SA_s$. Using intuition from the federated learning community [30], we define the upper bound of SA_s as the set of models retrained using all combinations the powerset of N , $\mathbb{P}(N)$. This gives us latitude in selecting optimal models, but provides resource challenges for large swarms. The Fleet Computer provides developers the option to provide heuristics to prune aggregators from SA_s , and can use usefulness to prune SA_s online. It is unclear a priori how each model in SA_s will affect each swarm member, so training effects must be determined online. Therefore, we track a series of performance-based system level hyper-parameters.

We track model weights $\{U_w^1..U_w^i\}$ for models $\{SA_1..SA_i\} \in SA_s$. Model weights describe the weighted percentage ($0 \leq U_w^x \leq 1$, $\sum_{n=1}^i U_w^n = 1$) that decisions from that model are incorporated into a pathfinding decisions. The goal of our approach is to determine the values for these hyperparameters which yield us the best mission performance. Per swarm member, we define these hyperparameters as x .

$$x = \{U_w^1, U_w^2, \dots, U_w^i\} \quad (14)$$

$SA_s(x)$ describes the Fleet Computer mission whose pathfinding decisions for a single agent are determined by SA_s weighted by x . The Fleet Computer’s goal is to determine a set of hyperparameters x^* that best accomplishes autonomy goals. More specifically, we want to optimize the following objective function.

$$x^* = x \text{ s.t. } \operatorname{argmax}(Eval(SA_s(x)) | SA_s(x) > G) \quad (15)$$

We use $Eval(SA_s(x))$ representing the evaluation of a full mission informed by $SA_s(x)$. Our goal is to find x^* , the set of weights that maximize the evaluation, while assuring that our autonomy goals G are met.

Bayesian optimization [18, 40] is a powerful technique often used in hyperparameter tuning to improve machine learning algorithms performance. Bayesian optimization works well for optimization problems where objective functions are derivative free, expensive to evaluate, noisy, lack structures that are easy to optimize, and have small parameter sets [18]. Reinforcement learning approaches often fit all of these criteria, ours included. To optimize our hyperparameters, we use expected improvement to quickly minimize our objective function given specified goals. Expected improvement approximates the global maximum of our objective function by sampling hyperparameters based on the posterior distribution of prior sample points and loss. Expected improvement determines hyperparameter samples with a balance between the highest probability for improvement and the largest magnitude of that improvement. We model this as a Gaussian process.

The above approach frames Bayesian optimization in the scope of a single agent’s parameters, but we can use this approach to optimize hyperparameters for multiple agents. Using the same local-optimization approach, we can determine a near-optimal x to maximize global goals. Each swarm member maintains its own set of hyperparameters x_i which is updated asynchronously after each mission. The collective set of hyperparameters provides us a simple metric for determining how ‘useful’ each model in SA_s is to overall pathfinding decisions. Models with higher average U_w^i provide more insight into pathfinding decisions, and therefore should be updated more regularly and provided more retraining resources.

4.2 Scheduling and power management

The Fleet Computer consumes edge resources to support movement, actuation, pathfinding, data storage, and online learning. Within this set of activities it is important to balance the resource needs of critical real-time latency-sensitive processes, like movement control, with compute intensive tasks like retraining routines that offer significant long-term gain. It is also important for edge resources to be responsive

to workload changes, powering down edge devices in low load periods to maximize system liveness and mission length, and scaling out in peak loads to support effective decision-making. Here we describe our solutions to both of these challenges: Section 4.2.1 presents our priority-based container scheduling solution for latency-sensitive and compute-intensive tasks, which factors in utility of each compute-intensive training task to overall mission objectives, and Section 4.2.2 describes our cluster autoscaling mechanism to adjust to workload changes.

4.2.1 Priority-based Scheduling. The Fleet Computer deploys all of its core components in containers [37] to maintain hardware independence and support scale-out. Figure 1 shows the different container types that encapsulate pre-built inputs like MARL algorithms, retraining routines, and feature extractors along with core Fleet Computer platform elements.

Container scheduling across clusters is well understood [9]. We use Kubernetes [49] for automated bin-backing of containers across clusters, allocating resources for all Fleet Computer components defined as Docker containers. We use priority-based scheduling to ensure that latency-sensitive real-time tasks such as UAV flight control are assured to be executable within their latency window; we then use additional edge compute to schedule model retraining tasks based on newly-received data from swarm members of the in-progress mission.

For model retraining tasks, we augment the resource allocation algorithm used by Kubernetes to optimise *placement* and *task selection* for Fleet Computer operations. Placement decisions are impacted by data locality, where training data for SA and HA models is typically fragmented across multiple systems within the Fleet Computer. Our resource allocation algorithm guarantees that containers will be scheduled on an edge node that either (1) has at least some of the data required for model retraining, or (2) is within a user-defined edge hub with expanded compute. This provides Kubernetes with sufficient flexibility in scheduling, but guarantees that data transfer times remain relatively low and allows for the potential of partial or complete data locality at the training site.

Task selection is impacted by the likely utility of a retraining task: when edge compute resources cannot support all retraining tasks, we choose those with the highest average utility. The Fleet Computer uses Kubernetes’ priority scheme for scheduling training procedures using the aggregate usefulness of each model provided by AS containers as shown in Figure 4. Model usefulness is simply the floating point value $U_i = [0, 1]$ assigned by Bayesian optimization, as explained in Section 4.1. If model usefulness is calculated by multiple swarm members, usefulness is weighted evenly among them. Scheduler priority for model i is then:

$$P_i = \lfloor 10 * U_i \rfloor * 100,000,000 \quad (16)$$

P_i then becomes a priority value in range $[0..900,000,000]$ at intervals of 100,000,000, allowing for 10 possible priority values. This range maps into the entire range of priority levels available in Kubernetes, which is specified by integers between 0 and 1 billion, while providing a coarse granularity that clearly differentiates retraining routines of different utilities and allows us to reserve the priority level 10 for sensor containers.

We also use usefulness to assign compute resources. Kubernetes allows users to provide minimum and maximum resource usage constraints when pods are instantiated. We use the same priority numbers $[0, 9]$ to assign relative CPU and RAM maximums to pods. All available RAM and CPU units are portioned among pods based on their priority levels.

$$CPU_i = \frac{CPU_t}{\sum_{j=0}^s P_j} * P_i \quad (17)$$

Shown above, all CPU cores available across the system CPU_t for retraining are split evenly among pods based on priority. This same process is used to allocate memory. Pods with a priority of 0 are not scheduled. This priority mechanism allows us to provide more resources to retrain models that agents consider useful, and avoid retraining models that provide little to the system.

4.2.2 Cluster Autoscaling. Because Fleet Computers may include many nodes, and edge devices in particular are likely to be provisioned for peak loads rather than average load, it is beneficial to regularly scale the cluster up and down in response to workloads.

The Fleet Computer includes a custom Kubernetes autoscaler which drains compute tasks from superfluous nodes and powers them down, saving on edge power when loads are low, and re-powers decommissioned nodes using Wake-On-LAN [38] when the system detects that more compute will soon be required.

Powering down nodes in this way must be sensitive to cluster storage implications. Each edge node stores different fragments of data, so we must ensure that no data becomes unavailable. For this purpose we use the Hadoop Distributed File System (HDFS) [51] for cluster data management, configured to replicate all data twice across the edge node cluster. When data is ‘lost’ from a decommissioned node it will therefore still be available at one other node in the cluster; after each decommission we simply wait for data to be re-replicated by HDFS before powering down any further nodes, guaranteeing data availability as the active node population changes.

5 Applications

We use two very different application types to help evaluate the Fleet Computer: one using a swarm of crop scouting UAVs, and one using a swarm of taxi tracking cameras.

Our crop scouting swarm builds on prior work [66] where UAVs navigate a corn field and capture images which are used to construct a yield map as outlined in Section 2. Farmers use yield maps to inform crop management strategies like fungicide, pesticide, and herbicide application. Large crop fields may cover hundreds of acres, requiring days of swarm coverage and human labor to gather a complete yield map. Prior work used reinforcement learning to creatively sample fields, covering a fraction of the field autonomously and predicting the rest. This approach creates usable yield maps in a fraction of the time at lower cost, but requires considerable developer effort. Actions in the crop scouting application are UAV direction movements, in a field which is divided into a grid. In this application we used the same dataset of corn images as prior work, consisting of 684 UAV sensed 4608x3456 images of a corn field in London, Ohio. We input the same Q-learning based model and feature extraction from prior work into the fleet spec as SA and $Map()$, and modified the extrapolation function from prior work which generated crop yield maps to produce an $Eval()$, which provides goal information like edge and UAV energy along with overall map accuracy. We used the Fleet Computer’s reward shaping mechanism to build reward and distance functions, defining state-groups as unique 3x3 regions of states.

Our taxi tracking swarm also builds on prior work in video analytics [24]. Spatula is a cross-camera video analytics framework: for a specific target (a person, taxi, etc) in one video stream, it returns all frames across all cameras which contain that target. Spatula avoids searching all cameras by searching only cameras that are highly spatially and temporally correlated. Spatula builds these correlation matrices offline using prior execution data. Online, cameras are only searched if their spatial and temporal correlation scores are higher than user-provided thresholds. This approach performs considerably better than searching all cameras and frames, but runs the risk of staleness as movement patterns change over time, and also requires users to manually determine threshold values. To implement this application we used the Porto Taxi Service Trajectory dataset [42], also used to test Spatula. Similar to the original implementation, we generated spatial and temporal correlations using 130 virtual cameras pinned in an evenly spaced grid within Porto, Portugal. Correlation matrices were provided to the Fleet Spec as the State-to-Action model, and trajectories from the Porto data set were provided in place of $Map()$. We built a custom $Eval()$ function which reports overall accuracy and the total number of frames checked for targets throughout execution, and we generated an HA function to determine optimal temporal and spatial thresholds. We defined state-groups as 50% overlapped 1-minute sets of video frames from each camera.

Online learning for both systems consists of retraining models and rebuilding reward and distance functions using recently received execution data. For crop scouting, swarm sizes were small, so we dispatched $\mathbb{P}(N)$ aggregators for retraining after every crop-scouting mission (i.e when a swarm generates a final yield map). For Spatula, swarm sizes are large, so we dispatched N aggregators after every simulated day to rebuild correlation matrices and relearned thresholds.

6 Evaluation

We implemented swarms for both applications described in Section 5 using multiple competing approaches. In this section, we describe our experimental testbed and then evaluate the efficacy and performance of Fleet Computer swarms.

6.1 Architecture

The Fleet Computer is designed for edge deployments. Our canonical prototype uses 6 total machines, comprising 5 consumer laptops as gateways and a server as an edge hub. Consumer laptops include 3 HP 250 G6 laptops with i5 CPUs and 8GB RAM and two Lenovo Thinkpad T470s with i7 CPUs and 8GB RAM. The server includes an i9 CPU, 32GB RAM, and an Nvidia RTX 3080 GPU. Each machine runs Ubuntu 20.04 Linux. All systems in the Fleet Computer are connected by Ethernet to a 10 Gbps Netgear router.

The Fleet Computer uses one of the Lenovo Thinkpads as a master node to control Kubernetes, Docker, and HDFS. The master node also runs a custom Kubernetes governor, a collection of daemons that create the Kubernetes cluster, start autonomous missions, automatically allocate and prioritize retraining containers, autoscale the cluster, and duty-cycle other machines. When retraining occurs, containers are scheduled by the governor as pods in the Kubernetes cluster. Each pod is scheduled based on its aggregate usefulness as determined by all swarm members as discussed in Section 5.

For our crop scouting application, DJI Mavics provide the base UAV characteristics for emulation. Each UAV in a swarm is assigned an HP or Lenovo laptop as a gateway for communication with the Fleet Computer. The UAV’s control software runs in a container on the gateway. To gather crop scouting results, we simulated UAV by replaying data captured from previous missions. All UAV control software executed as it would in the field, but data was provided by software. This allowed us to execute all UAV commands without flying, but receive appropriate execution data based on validated energy and latency models [6].

6.2 Results

We evaluate the Fleet Computer’s comparative performance against state-of-the-art swarm control, the effectiveness of our runtime scheduling approach in saving energy on edge devices, and the effectiveness of our online learning approach

at autonomously selecting effective data aggregations for retraining on our resource-constrained edge devices.

Figure 5 (a-b) shows the Fleet Computer’s performance on our crop scouting and video analytics workloads *without* additional online learning. For crop scouting, we compare against the state of the art in prior work [66] (*Classic RL*) which utilized Q-learning to map crop fields. We test the Fleet Computer against classic RL using 3 swarm sizes (1, 2, and 4 UAVs), and two autonomy goals: one seeking high-accuracy (>90%) maps; and the other prioritizing throughput, accepting 70% accurate maps in exchange for fast sampling. Both approaches started with the same Q-learning State-to-Action model, but the Fleet Computer generates its own History-to-Action model and reward function from experience.

For the both accuracy conditions, the Fleet Computer decreased mission length by 10-75% compared to Classic RL. Using a swarm of 4 UAVs, compared to a single UAV as used in prior work, we observe a mission length decrease of 3.9-4.4X. This decrease is in part due to having more UAVs, but represents more than 4x the performance gain due to the Fleet Computer’s intelligent mission learning and redesign.

Figure 5(e) shows why Fleet Computer missions complete more quickly – compared against both a Classic RL and current-industry-practice automated search which scouts waypoints linearly, row by row until the coverage goal is reached [3, 23]. The Fleet Computer consistently outperforms both prior approaches, most notably at lower accuracy goals, by sampling an average of just 26% of a crop field to generate a 70% accurate yield map, improving over Classic RL and automated by 1.73X and 2.2X respectively. These improvements are gained because the Fleet Computer learns from experience which areas of a field are likely to be similar to adjacent regions and so do not need detailed data capture.

Figure 5(b) shows the Fleet Computer’s performance against Spatula. Spatula uses a shared correlation matrix and a single controller to implement cross-camera analysis, and so is only shown in the ‘1’ category on Figure 5(b). The Fleet Computer enables us to easily model cross-camera analytics as a distributed swarm of cameras, where each agent is provided compute resources to respond to global queries across one or more cameras. Using this approach, the Fleet Computer can highly parallelize query response and so offers very large potential performance gains without complex programming. We used the Fleet Computer’s History-to-Action model to automatically set Spatula’s spatial and temporal thresholds, and tested performance by swarm size and for high throughput and high accuracy goals. Our experiments examine performance gains at increasing numbers of swarm agents applied to the same problem, which is easy to configure through the Fleet Computer; at the highest number of 130 swarm agents we found that the Fleet Computer can parallelize Spatula’s workload highly effectively, processing queries 39X and 62X faster than the single Spatula controller.

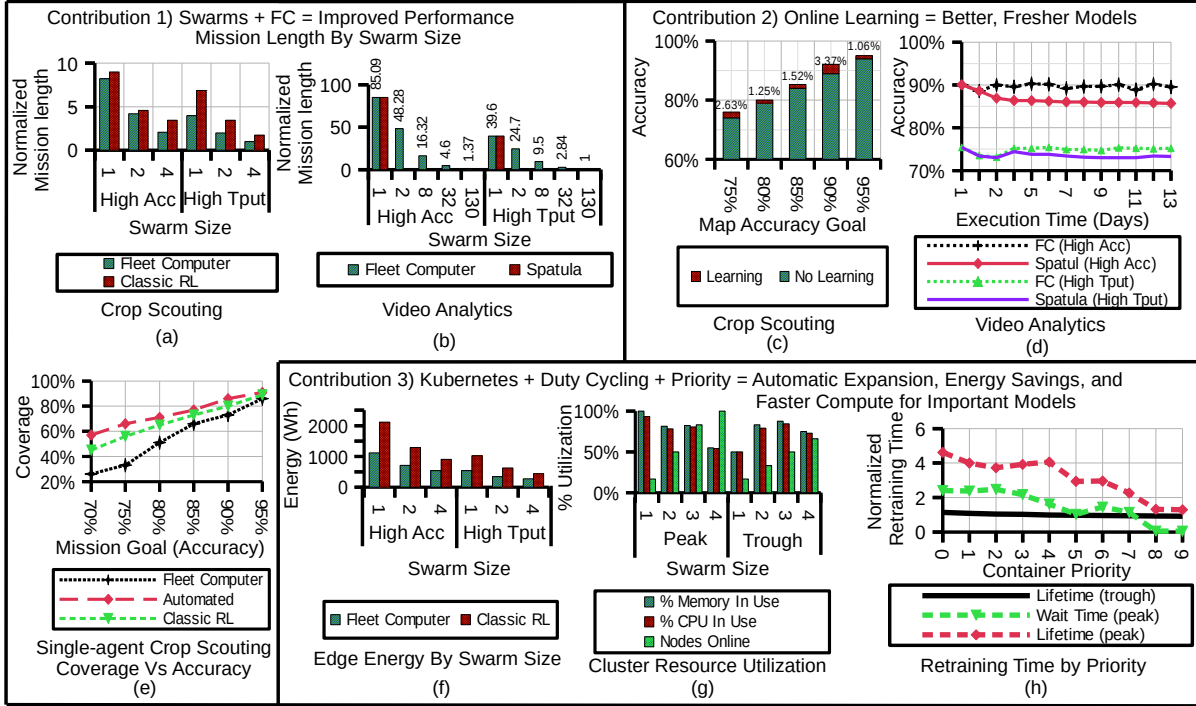


Fig. 5. Experimental results: a,b,e) The Fleet Computer’s programming model and swarm capabilities improve performance considerably, c-d) Online learning keeps models fresh and helps adapt to new execution contexts, f-h) The Fleet Computer’s system management features save energy and improve performance by duty cycling hardware, expanding compute efficiently, and prioritizing high-value model updates.

When we introduce *online learning* to these scenarios we see further improvements for both applications. Figures 5(c) and (d) show how crop-scouting can improve over time, and how regularly updating HA models can maintain Spatula’s performance as movement patterns evolve.

Figure 5(c) shows how online learning improves crop scouting accuracy. In this experiment we run 10 successive real-time swarm missions across simulated crop fields, allowing online learning to continually improve models across a 4 UAV swarm for accuracy goals between 75% and 95%. By the 10th mission we see that every condition moves closer to its target accuracy level by between 1% and 3%; if we measure this as decrease in relative model error from the target accuracy this equates to between 5% and 28% improvement. These savings improve accuracy goals with no increase in resource requirements or mission lengths.

Figure 5(e) shows that Spatula’s performance with retraining remains consistent with autonomy goals if retrained, but degrades quickly without retraining. We trained Spatula on one day of Porto Taxi Data using all 130 cameras and 448 Taxis, then examined its performance compared to the Fleet Computer on each following day of a two-week period after its initial training. For both high accuracy and high throughput goals, the Fleet Computer remains consistent (within 1%) with accuracy goals. Spatula, in both cases, consistently

under-performs accuracy goals after 2 and 4 days for high accuracy and throughput respectively. At the end of the two week period, the Fleet Computer outperforms Spatula by 5% and 3% for high accuracy and throughput respectively by maintaining fresh models.

We next examine the Fleet Computer’s resource management approach and its effect on edge site energy usage. Figures 5(f-h) show how the Fleet Computer’s edge-focused Kubernetes runtime improves overall edge performance on our crop scouting benchmark. Using the prototype Fleet Computer, we ran 10 real-time crop scouting missions for each swarm setting using UAV-collected data with modeled UAV movement, timings, and data-transfer provided by prior work [6]. Energy was calculated using an AC watt meter. We tested 1, 2, and 4 drone swarms with both high accuracy and high throughput goals. Figure 5(f) shows the Fleet Computer’s performance against Classic RL in terms of energy consumption. The Fleet Computer conserves energy in two different ways: mission lengths are shorter overall, and use of edge sites during a missing is cheaper due to automated power-down of resources in non-peak load periods. Compared to Classic RL, similar sized Fleet Computer missions consume 1.58X-2X less power. A swarm of multiple UAVs is also more energy efficient per-device than fewer UAVs; compared to Classic RL using a single UAV as in prior

work, a swarm of four fleet-computer-controlled UAVs uses 3.7X-3.9X less energy depending on swarm size and goals.

Figure 5(g) shows how the Fleet Computer manages resources across extremes during a swarm mission. For a single UAV, one node of the Fleet Computer cluster is enough to handle all resource needs. As the swarm grows, more nodes must be provisioned. As nodes increase from 2 to 4, peak and trough allocation change. For instance, a 4-UAV swarm can operate at troughs using just 4 nodes, but requires all 6 to handle peak loads. The Fleet Computer’s energy savings shown in Figure 5(f) are a direct result of its ability to spread resources evenly across the cluster and shut down unnecessary nodes until they are needed.

Finally, we examine the Fleet Computer’s usefulness-aware model retraining; this offers better use of finite edge resources by selecting which training tasks are likely to yield the highest benefit to an ongoing mission. Figure 5(h) shows how our usefulness metric affects model retraining times compared to average retraining times. When the system is not under load, Kubernetes is easily able to distribute containers across it. If the system is correctly provisioned for the edge, however, it may experience peak loads where containers must contend for resources. We evaluated retraining times for 4-UAV on our crop-scouting benchmark. We found that wait-times for high-priority containers (8-9 on the x-axis) were insignificant even at peak loads, but could be up to 2.4X normal retraining time for very low (0-2) priority containers. Similarly, high-priority containers experienced only modest (1.3X) lifetime increases even when the system was highly pressured. This was at the expense of lower priority containers, which experienced lifetimes up to 4.6X longer than usual. This behavior allows the system to take resources from models with low utility to the system and give them to high utility models.

6.3 Limitations and Future Work

The Fleet Computer uses Bayesian optimization for reward shaping, online learning and scheduling. While Bayesian optimization has admirable attributes, like fast convergence, other popular techniques, such as gradient descent, could be applied as well. We have not explored the tradeoffs in convergence time and learning efficacy. HA models leverage spatial properties that most MARL algorithms do not, but our approach is relatively simple. A more complex model could further reduce unneeded actions, but may also increase training and inference times. In particular, FlexDNN provides a rigorous analysis of similar early-exit models in DNN frameworks [17]. We evaluated two applications that are analogous to Q-learning. Future work could explore deep Q-networks increasingly used in autonomous systems. Finally, while we used real hardware and workloads in our evaluation, we simulated data capture from edge devices and did not explore swarms bottlenecked by data ingestion.

7 Related Work

Much recent work has dealt with tackling the concerns of real-world autonomous systems using strong theoretical foundations. Lin et al [32] explores a federated meta-learning approach to train models with small datasets in an edge setting. Singh et. al [54] demonstrates a novel reward-training mechanism for reinforcement learning to eliminate the need for reward shaping. Kilinc and Montana [29] constructs a framework for sharing data among agents in execution contexts that are noisy and non-stationary using intrinsic reward and temporal locality. Other recent work [46, 63, 65] on networked agents provide considerable insight into the behaviors of real-world cooperative MARL systems with limited communication capabilities. Porter et. al [45] presents a novel development platform for creating software that autonomously assembles itself and discovers optimal execution policies online without the need for expert model building and reward shaping.

Much related work deals specifically with autonomous aerial systems. Boubin et. al [6] demonstrates that naive hardware and algorithm selection for fully autonomous aerial systems can have serious performance consequences. Cui et. al [11] implements MARL for allocating networking resources across a network of UAV base-stations. In agriculture Zhang et. al [66], Yang et. al [60], and FarmBeats [57] provide new techniques for automated and autonomous UAV crop scouting.

8 Conclusion

Swarms of autonomous systems powered by resources at the edge can provide insight and actuation that will revolutionize industries like agriculture, construction, transportation, and video analytics. We present the Fleet Computer, an end-to-end platform for building, deploying, and executing swarms. To use the Fleet Computer, developers implement *Map()* and *Eval()* functions and specify mission configurations. The Fleet Computer compiles and deploys swarms using a multi-agent reinforcement learning framework. At runtime, the Fleet Computer manages data aggregation between swarm members, linking online learning outcomes to the efficient management of edge resources. Our evaluation showed that the Fleet Computer can produce effective and efficient swarms, suggesting this tool chain could make swarms accessible to everyday developers.

References

- [1] A. Al-Kaff, F. M. Moreno, L. J. San José, F. García, D. Martín, A. de la Escalera, A. Nieva, and J. L. M. Garcéa. Vbii-uav: Vision-based infrastructure inspection-uav. In *World Conference on Information Systems and Technologies*, pages 221–231. Springer, 2017.
- [2] Amazon. Prime air. <https://www.amazon.com/Amazon-Prime-Air/b?ie=UTF8&node=8037720011>, 2020.
- [3] A. Barrientos, J. Colorado, J. d. Cerro, A. Martinez, C. Rossi, D. Sanz, and J. Valente. Aerial remote sensing in agriculture: A practical approach to area coverage and path planning for fleets of mini aerial robots.

- Journal of Field Robotics*, 28(5):667–689, 2011.
- [4] E. Bastug, M. Bennis, M. Médard, and M. Debbah. Toward interconnected virtual reality: Opportunities, challenges, and enablers. *IEEE Communications Magazine*, 55(6):110–117, 2017.
 - [5] J. Boubin, J. Chumley, C. Stewart, and S. Khanal. Autonomic computing challenges in fully autonomous precision agriculture. In *2019 IEEE International Conference on Autonomic Computing (ICAC)*. IEEE, 2019.
 - [6] J. G. Boubin, N. T. Babu, C. Stewart, J. Chumley, and S. Zhang. Managing edge resources for fully autonomous aerial systems. In *Proceedings of the 4th ACM/IEEE Symposium on Edge Computing*, pages 74–87. ACM, 2019.
 - [7] A. Bouman, M. F. Ginting, N. Alatur, M. Palieri, D. D. Fan, T. Touma, T. Pailevanian, S.-K. Kim, K. Otsu, J. Burdick, et al. Autonomous spot: Long-range autonomous exploration of extreme environments with legged locomotion. *arXiv preprint arXiv:2010.09259*, 2020.
 - [8] L. Busoni, R. Babuska, and B. De Schutter. A comprehensive survey of multiagent reinforcement learning. *IEEE Transactions on Systems, Man, and Cybernetics, Part C (Applications and Reviews)*, 38(2):156–172, 2008.
 - [9] E. Casalicchio. Container orchestration: A survey. In *Systems Modeling: Methodologies and Tools*, pages 221–235. Springer, 2019.
 - [10] Y.-h. Chang, T. Ho, and L. Kaelbling. All learning is local: Multi-agent learning in global reward games. *Advances in Neural Information Processing Systems*, 16:807–814, 2003.
 - [11] J. Cui, Y. Liu, and A. Nallanathan. Multi-agent reinforcement learning-based resource allocation for uav networks. *IEEE Transactions on Wireless Communications*, 19(2):729–743, 2019.
 - [12] M. De Deuge, A. Quadros, C. Hung, and B. Douillard. Unsupervised feature learning for classification of outdoor 3d scans. In *Australasian Conference on Robotics and Automation*, volume 2, page 1, 2013.
 - [13] J. Dean and S. Ghemawat. Mapreduce: simplified data processing on large clusters. *Communications of the ACM*, 51(1):107–113, 2008.
 - [14] T. Doan, S. Maguluri, and J. Romberg. Finite-time analysis of distributed td (0) with linear function approximation on multi-agent reinforcement learning. In *International Conference on Machine Learning*, pages 1626–1635. PMLR, 2019.
 - [15] M. Faessler, F. Fontana, C. Forster, E. Mueggler, M. Pizzoli, and D. Scaramuzza. Autonomous, vision-based flight and live dense 3d mapping with a quadrotor micro aerial vehicle. *Journal of Field Robotics*, 33(4), 2016.
 - [16] F. Fahimi. Autonomous robots. *Modeling, Path Planning and Control*, 2009.
 - [17] B. Fang, X. Zeng, F. Zhang, H. Xu, and M. Zhang. Flexdnn: Input-adaptive on-device deep learning for efficient mobile vision. In *Proceedings of the 5th ACM/IEEE Symposium on Edge Computing (SEC)*, 2020.
 - [18] P. I. Frazier. A tutorial on bayesian optimization. *arXiv preprint arXiv:1807.02811*, 2018.
 - [19] A. Geiger, P. Lenz, C. Stiller, and R. Urtasun. Vision meets robotics: The kitti dataset. *The International Journal of Robotics Research*, 32(11):1231–1237, 2013.
 - [20] I. Grondman, L. Busoni, G. A. Lopes, and R. Babuska. A survey of actor-critic reinforcement learning: Standard and natural policy gradients. *IEEE Transactions on Systems, Man, and Cybernetics, Part C (Applications and Reviews)*, 42(6):1291–1307, 2012.
 - [21] M. Grzes. Reward shaping in episodic reinforcement learning. In *Proceedings of the 16th Conference on Autonomous Agents and MultiAgent Systems*, pages 565–573, 2017.
 - [22] N. Hassan, K.-L. A. Yau, and C. Wu. Edge computing in 5g: A review. *IEEE Access*, 7:127276–127289, 2019.
 - [23] J. Hu, A. Bruno, B. Ritchken, B. Jackson, M. Espinosa, A. Shah, and C. Delimitrou. Hivemind: A scalable and serverless coordination control platform for uav swarms. *arXiv preprint arXiv:2002.01419*, 2020.
 - [24] S. Jain, X. Zhang, Y. Zhou, G. Ananthanarayanan, J. Jiang, Y. Shu, P. Bahl, and J. Gonzalez. Spatula: Efficient cross-camera video analytics on large camera networks. In *2020 IEEE/ACM Symposium on Edge Computing (SEC)*, pages 110–124. IEEE, 2020.
 - [25] S. Kar, J. M. Moura, and H. V. Poor. Qd-learning: A collaborative distributed strategy for multi-agent reinforcement learning through consensus + innovations. *IEEE Transactions on Signal Processing*, 61(7):1848–1862, 2013.
 - [26] S. Kato, E. Takeuchi, Y. Ishiguro, Y. Ninomiya, K. Takeda, and T. Hamada. An open approach to autonomous vehicles. *IEEE Micro*, 35(6), 2015.
 - [27] R. Kesten, M. Usman, J. Houston, T. Pandya, K. Nadhamuni, A. Ferreira, M. Yuan, B. Low, A. Jain, P. Ondruska, S. Omari, S. Shah, A. Kulkarni, A. Kazakova, C. Tao, L. Platinsky, W. Jiang, and V. Shet. Lyft level 5 perception dataset 2020. <https://level5.lyft.com/dataset/>, 2019.
 - [28] S. Khanal, J. Fulton, N. Douridas, A. Klopfenstein, and S. Shearer. Integrating aerial images for in-season nitrogen management in a corn field. *computers and electronics in agriculture*, 148, 2018.
 - [29] O. Kilinc and G. Montana. Multi-agent deep reinforcement learning with extremely noisy observations. *arXiv preprint arXiv:1812.00922*, 2018.
 - [30] J. Konečný, H. B. McMahan, D. Ramage, and P. Richtárik. Federated optimization: Distributed machine learning for on-device intelligence. *arXiv preprint arXiv:1610.02527*, 2016.
 - [31] T. P. Lillicrap, J. J. Hunt, A. Pritzel, N. Heess, T. Erez, Y. Tassa, D. Silver, and D. Wierstra. Continuous control with deep reinforcement learning. *arXiv preprint arXiv:1509.02971*, 2015.
 - [32] S. Lin, G. Yang, and J. Zhang. A collaborative learning framework via federated meta-learning. In *2020 IEEE 40th International Conference on Distributed Computing Systems (ICDCS)*, pages 289–299. IEEE, 2020.
 - [33] S.-C. Lin, Y. Zhang, C.-H. Hsu, M. Skach, M. E. Haque, L. Tang, and J. Mars. The architectural implications of autonomous driving: Constraints and acceleration. In *ASPLoS*, 2018.
 - [34] X. V. Lin, R. Socher, and C. Xiong. Multi-hop knowledge graph reasoning with reward shaping. *arXiv preprint arXiv:1808.10568*, 2018.
 - [35] M. L. Littman. Markov games as a framework for multi-agent reinforcement learning. In *Machine learning proceedings 1994*, pages 157–163. Elsevier, 1994.
 - [36] MarketDataForecast. Self-driving cars market. <https://www.marketdataforecast.com/market-reports/self-driving-cars-market>, 2020.
 - [37] D. Merkel. Docker: lightweight linux containers for consistent development and deployment. *Linux journal*, 2014(239):2, 2014.
 - [38] N. Mishra, K. Chebrolu, B. Raman, and A. Pathak. Wake-on-wlan. In *Proceedings of the 15th international conference on World Wide Web*, pages 761–769, 2006.
 - [39] V. Mnih, K. Kavukcuoglu, D. Silver, A. A. Rusu, J. Veness, M. G. Bellemaire, A. Graves, M. Riedmiller, A. K. Fidjeland, G. Ostrovski, et al. Human-level control through deep reinforcement learning. *nature*, 518(7540):529–533, 2015.
 - [40] J. Mockus and L. Mockus. Bayesian approach to global optimization and application to multiobjective and constrained problems. *Journal of Optimization Theory and Applications*, 70(1):157–172, 1991.
 - [41] N. Mohan, L. Corneo, A. Zavodovski, S. Bayhan, W. Wong, and J. Kangasharju. Pruning edge research with latency shears. In *Proceedings of the 19th ACM Workshop on Hot Topics in Networks*, pages 182–189, 2020.
 - [42] L. Moreira-Matias, J. Gama, M. Ferreira, J. Mendes-Moreira, and L. Damas. Predicting taxi-passenger demand using streaming data. *IEEE Transactions on Intelligent Transportation Systems*, 14(3):1393–1402, 2013.
 - [43] D. Munoz, J. A. Bagnell, N. Vandapel, and M. Hebert. Contextual classification with functional max-margin markov networks. In *2009 IEEE Conference on Computer Vision and Pattern Recognition*, pages 975–982. IEEE, 2009.

- [44] M. Pfeiffer, M. Schaeuble, J. Nieto, R. Siegwart, and C. Cadena. From perception to decision: A data-driven approach to end-to-end motion planning for autonomous ground robots. In *2017 IEEE International Conference on Robotics and Automation (ICRA)*, pages 1527–1533. IEEE, 2017.
- [45] B. Porter, M. Grieves, R. Rodrigues Filho, and D. Leslie. Rex: A development platform and online learning approach for runtime emergent software systems. In *Symposium on Operating Systems Design and Implementation*, pages 333–348. USENIX, November 2016.
- [46] G. Qu, A. Wierman, and N. Li. Scalable reinforcement learning of localized policies for multi-agent networked systems. In *Learning for Dynamics and Control*, pages 256–266, 2020.
- [47] R. Raj, J. P. Walker, R. Pingale, R. Nandan, B. Naik, and A. Jagarlapudi. Leaf area index estimation using top-of-canopy airborne rgb images. *International Journal of Applied Earth Observation and Geoinformation*, 96:102282, 2021.
- [48] J. L. Sanchez-Lopez, R. A. S. Fernández, H. Bavle, C. Sampedro, M. Molina, J. Pestana, and P. Campoy. Aerostack: An architecture and open-source software framework for aerial robotics. In *International Conference on Unmanned Aircraft Systems*, 2016.
- [49] G. Sayfan. *Mastering kubernetes*. Packt Publishing Ltd, 2017.
- [50] E. Semsch, M. Jakob, D. Pavlicek, and M. Pechoucek. Autonomous uav surveillance in complex urban environments. In *2009 IEEE/WIC/ACM International Joint Conference on Web Intelligence and Intelligent Agent Technology*, volume 2, pages 82–85. IEEE, 2009.
- [51] K. Shvachko, H. Kuang, S. Radia, and R. Chansler. The hadoop distributed file system. In *2010 IEEE 26th symposium on mass storage systems and technologies (MSST)*, pages 1–10. Ieee, 2010.
- [52] R. Siegwart, I. R. Nourbakhsh, and D. Scaramuzza. *Introduction to autonomous mobile robots*. MIT press, 2011.
- [53] N. Silberman, D. Hoiem, P. Kohli, and R. Fergus. Indoor segmentation and support inference from rgb-d images. In *European conference on computer vision*, pages 746–760. Springer, 2012.
- [54] A. Singh, L. Yang, K. Hartikainen, C. Finn, and S. Levine. End-to-end robotic reinforcement learning without reward engineering. *arXiv preprint arXiv:1904.07854*, 2019.
- [55] Z. Sui, Z. Zhou, Z. Zeng, and O. C. Jenkins. Sum: Sequential scene understanding and manipulation. In *2017 IEEE/RSJ International Conference on Intelligent Robots and Systems (IROS)*, pages 3281–3288. IEEE, 2017.
- [56] C. Urmson, J. Anhalt, D. Bagnell, C. Baker, R. Bittner, M. Clark, J. Dolan, D. Duggins, T. Galatali, C. Geyer, et al. Autonomous driving in urban environments: Boss and the urban challenge. *Journal of Field Robotics*, 25(8):425–466, 2008.
- [57] D. Vasisht, Z. Kapetanovic, J. Won, R. Chandra, A. Kapoor, S. Sinha, M. Sudarshan, and S. Strätman. Farmbeats: An iot platform for data-driven agriculture. In *NSDI*, 2017.
- [58] S. Wan, J. Lu, P. Fan, and K. B. Letaief. Toward big data processing in iot: Path planning and resource management of uav base stations in mobile-edge computing system. *IEEE Internet of Things Journal*, 7(7):5995–6009, 2019.
- [59] C. J. Watkins and P. Dayan. Q-learning. *Machine learning*, 8(3-4):279–292, 1992.
- [60] M.-D. Yang, J. G. Boubin, H. P. Tsai, H.-H. Tseng, Y.-C. Hsu, and C. C. Stewart. Adaptive autonomous uav scouting for rice lodging assessment using edge computing with deep learning edanet. *Computers and Electronics in Agriculture*, 179:105817, 2020.
- [61] F. Yu, H. Chen, X. Wang, W. Xian, Y. Chen, F. Liu, V. Madhavan, and T. Darrell. Bdd100k: A diverse driving dataset for heterogeneous multitask learning. In *Proceedings of the IEEE/CVF conference on computer vision and pattern recognition*, pages 2636–2645, 2020.
- [62] C. Zhang and J. M. Kovacs. The application of small unmanned aerial systems for precision agriculture: a review. *Precision agriculture*, 13(6):693–712, 2012.
- [63] K. Zhang, Z. Yang, and T. Basar. Networked multi-agent reinforcement learning in continuous spaces. In *2018 IEEE Conference on Decision and Control (CDC)*, pages 2771–2776. IEEE, 2018.
- [64] K. Zhang, Z. Yang, and T. Başar. Multi-agent reinforcement learning: A selective overview of theories and algorithms. *arXiv preprint arXiv:1911.10635*, 2019.
- [65] K. Zhang, Z. Yang, H. Liu, T. Zhang, and T. Basar. Fully decentralized multi-agent reinforcement learning with networked agents. In *International Conference on Machine Learning*, pages 5872–5881. PMLR, 2018.
- [66] Z. Zhang, J. Boubin, C. Stewart, and S. Khanal. Whole-field reinforcement learning: A fully autonomous aerial scouting method for precision agriculture. *Sensors*, 20(22):6585, 2020.
- [67] Y. Zheng, Q. Li, Y. Chen, X. Xie, and W.-Y. Ma. Understanding mobility based on gps data. In *Proceedings of the 10th international conference on Ubiquitous computing*, pages 312–321, 2008.
- [68] Y. Zhou, B. Rao, and W. Wang. Uav swarm intelligence: Recent advances and future trends. *IEEE Access*, 8:183856–183878, 2020.
- [69] H. Zou, T. Ren, D. Yan, H. Su, and J. Zhu. Reward shaping via meta-learning. *arXiv preprint arXiv:1901.09330*, 2019.